RESEARCH OF INTEREST TO THE NASA RESEARCH AND TECHNOLOGY ADVISORY COMMITTEE ON MATERIALS AND STRUCTURES

March 25-26, 1976

NASA-Ames Research Center
Moffett Field, California

TABLE OF CONTENTS

TABLE OF CONTENTS

(Continued)

Aeronautical Structures Branch

1. FLEXSTAB Computer Program
2. Dynamic Loads Study
3. 2D Transonic Unsteady Aerodynamics
4. Nonsteady Loads Due to Buffet
5. Pressure Fluctuations Underlying Attached and Separated Turbulent Boundary Layers
6. Aero-Optical Interactions

FLEXSTAB Computer Program The NASA 1.02.00 version of FLEXSTAB is currently being prepared for delivery to COSMIC. The current estimate is that the CDC and IBM versions will be available from COSMIC by June 1 and August 1, 1976, respectively. COSMIC will release the code through a lease arrangement; the cost is expected to be $1750 for a ten-year lease. A requirement of the lease is that the leasee agrees to install the code only at his specific use location.

Approximately 40 sets of documentation (2000 pages per set) have been distributed from Ames since May 1975. The first of three sets of documentation update pages were distributed from Ames in February 1976; the second set will be distributed in March, 1976, and the third set about June, 1976. These updates represent changes required to make the documentation consistent with the 1.02.00 code that will be available from COSMIC.

If there are additional code and/or documentation changes, they will be distributed by COSMIC.

References

1. A Method for Predicting the Stability Characteristics of an Elastic Airplane.

   a. Vol. I - FLEXSTAB Theoretical Description, NASA CR 114712

   b. Vol. II - FLEXSTAB 1.02.00 User's Manual, NASA CR 114713

   c. Vol. III - FLEXSTAB 1.02.00 Program Description, NASA CR 114714

   d. Vol. IV - FLEXSTAB 1.02.00 Demonstration Cases and Results (available June, 1976), NASA CR 114715

2. Tinoco, E. N., and Mercer, J. E.: "FLEXSTAB - A Summary of the Functions and Capabilities of the NASA Flexible Airplane Analysis Computer Description",NASA CR-2564, December, 1975.

(Larry Erickson, FAS)

Dynamic Loads Study An assessment of the applicability of several aerodynamic methods to dynamic loads due to gusts and control surface motion has been performed under contract to The Boeing Company. The methods considered were:

(1) FLEXSTAB steady state aerodynamics

(2) Method '1' plus Kussner & Wagner functions

(3) FLEXSTAB steady and low frequency unsteady aerodynamics for predicting both the gust and moeion induced aerodynamic forces

(4) Method '3' with the low-frequency unsteady aerodynamic approximation not applied to the gust induced aerodynamic forces

(5) Strip theory plus wind tunnel corrections plus Kussner & Wagner functions

(6) The unsteady version of the vortex spline method

(7) The doublet-lattice method

(8) Rho's unsteady Kernel function method (used as the standard of comparison).

These methods were applied to a 747 modeled with an elastic wing but with all other components treated as rigid (e.g., fuselage, struts, nacelles). Discrete gusts, random atmospheric turbulence and an oscillating control surface were used as excitation sources.

From computed results for the aircraft transfer functions and power spectral density response it was concluded that:

(1) Methods '1' and '3' are inappropriate for dynamic loads analysis

(2) All the other methods are generally adequate for controls fixed gust analysis (because of gust power attenuation at higher frequencies).

(3) For active controls applications involving response at typical structural frequencies, the full unsteady methods (6, 7, 8) are required.

Although the three full unsteady methods predict essentially the same response for the discrete gust and atmospheric turbulence input, considerable disagreement exists between all three methods when the input is due to an oscillating aileron (see figures 1 and 2). The reason(s) for this disagreement are unknown. The differences raise the question as to which result is most correct and indicates the need for experimental correlations.

These results will be published in the near future in NASA CR-137720.

(Larry Erickson, FAS)

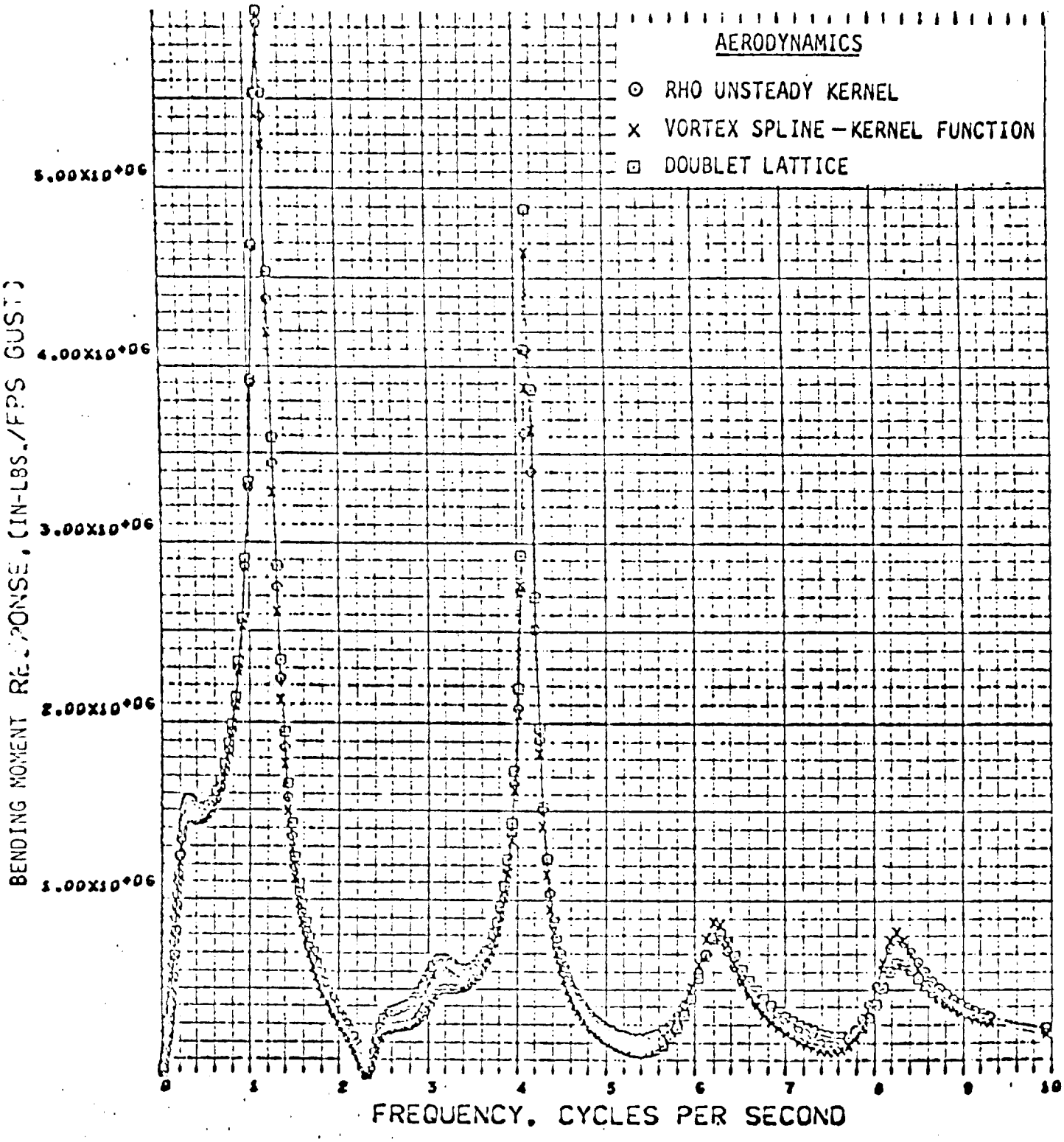

Wing B.M. Frequency Response at Wing Root Due to Gust Excitation

Fig. 1

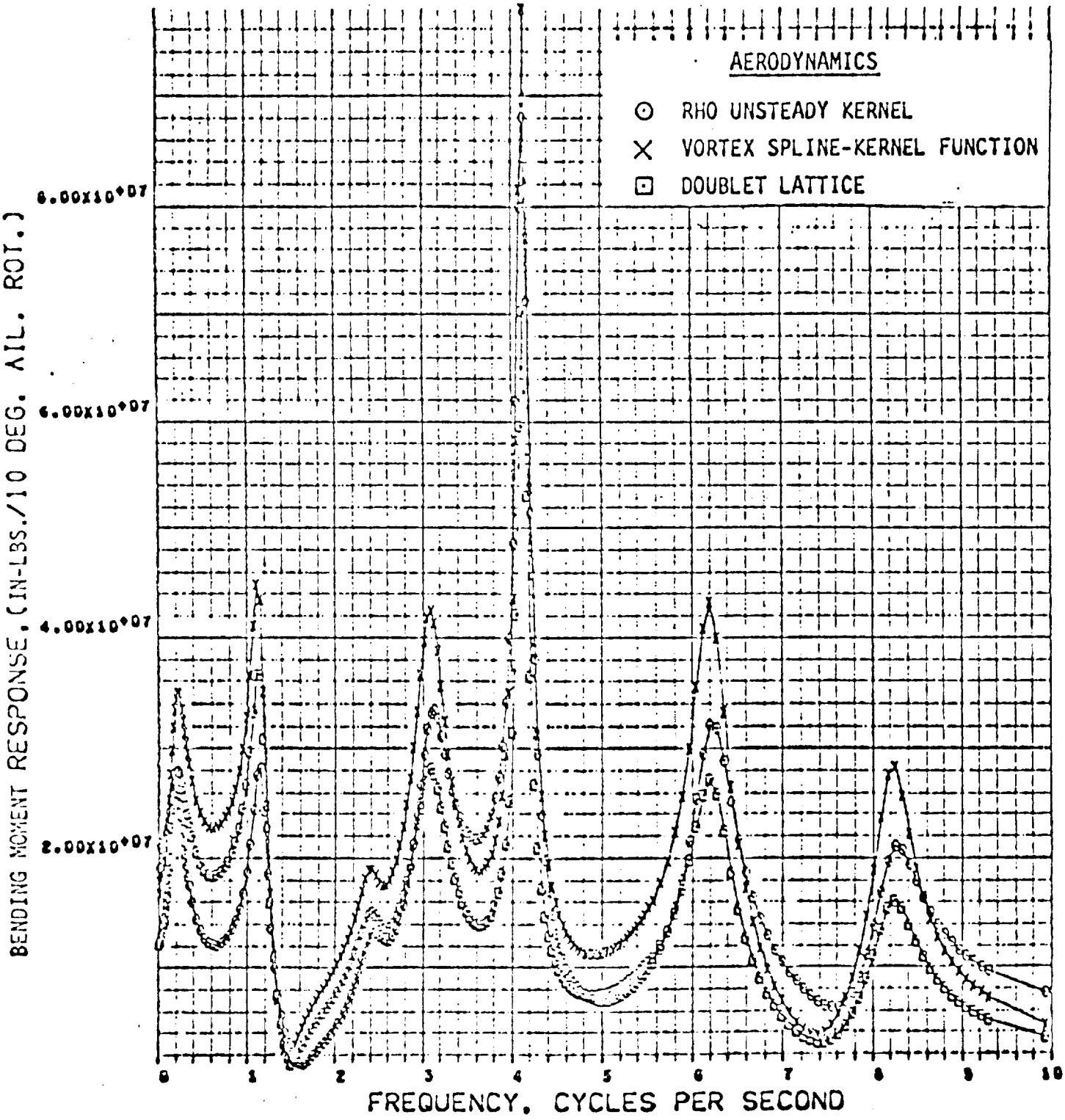

Wing B.M. Frequency Response at Wing Root Due To Oscillating Aileron Excitation

Fig. 2

2D Transonic Unsteady Aerodynamics Ames Research Center is participating in a cooperative program with LaRC and the AFFDL on the measurement and analysis of unsteady transonic flows. The purpose of the Ames effort is to measure the unsteady loading on rigid airfoils due to externally applied heaving and pitching motions. The broad objectives of this program are: (1) to understand the physics of unsteady transonic flows, (2) to validate existing and proposed numerical schemes, (3) to generate a data base for predicting the dynamic response of aerospace vehicles and (4) to develop new techniques for the measurement and analysis of unsteady phenomena.

The experimental effort at ARC will concentrate on 2D airfoil tests in the ARC 11- by 11-foot Transonic Wind Tunnel. A model support system for use in this wind tunnel is currently being designed. The system will consist of a pair of splitter plates spanning the test section in the vertical plane to form a 2D channel. Hydraulic actuators for driving the wing models are embedded in the splitter plates. The apparatus will be capable of oscillating airfoils (with or without control surfaces) with spans of 137 cm (54 in.) and chords up to 50 cm (20 in.) at frequencies up to 60 Hz. This yields a projected test envelope of reduced frequencies up to 0.30 (based on half-chord), Reynolds numbers up to 16×10^6 (based on chord), and a Mach number range of $0.40 \leq M_\infty \leq 1.4$.

In addition to the 11- by 11-ft tests, selected small scale testing is planned in conjunction with the construction of the 11- by 11-ft. test rig. One such test is an investigation into the validity of imposing the Kutta condition at the trailing edge of an oscillating airfoil. An initial investigation of trailing edge flows due to oscillating airfoils was completed during July and August of 1975. Professor R. A. Kadlec of the University of Colorado and S. Davis of ARC used the schlieren technique to visualize the streakline induced by a heated wire imbedded in an oscillating airfoil. These tests were made in a specially designed 25 x 35 cm quiet wind tunnel. The experiments were conducted at low subsonic speeds, but an effort is underway to convert this acoustic wind tunnel into a facility for the visualization of unsteady flows at transonic speeds. Further work is planned on unsteady flow visualization using laser interferometry and on the measurements of near wakes behind oscillating airfoils. Of course, all of these small scale experiments are conducted with the ultimate goal of understanding the physical phenomena in sufficient detail so that the large scale tests in the 11- by 11-foot wind tunnel can be performed in an efficacious and economical manner.

In order to determine the effect of forming a 2D channel in the test section of a transonic wind tunnel, another small scale test is planned for the winter of 1975-76. The ARC 2- by 2-ft. Transonic Wind Tunnel will be used to test an 18.2% scale model of the 11- by 11-ft. 2D channel. The starting loads on the channel walls will be measured and a pressure test will be performed on a fixed airfoil to assess the effect of channel geometry, wall porosity, etc. on the measured loading.

Results of the steady state test in the 2- by 2-ft. wind tunnel will be compared with a wide variety of numerical and analytical solutions to the transonic flow equations. The results of the unsteady tests will also be compared with available numerical and analytical solutions. A close liaison between the experimentalist and numerical analyst is being maintained throughout this program. The Computational Fluid Dynamics Branch at Ames, the Ames Directorate/AMRDL, contractual and inhouse work at AFFDL, as well as contracted and inhouse personnel

in the Aeronautical Structures Branch will contribute numerical solutions to certain baseline airfoil tests which will be conducted in the 11- by 11-ft. wind tunnel. Following the successful baseline tests, experiments on supercritical and other advanced technology airfoils are planned. At each stage critical comparisons will be made between the numerical, analytical and experimental results.

(S.Davis, FAS)

Nonsteady Loads Due to Buffet The NASA-Ames Research Center buffet intensity research program, as reported to previous meetings of this Committee, is continuing toward its objectives. Since the last reporting period, F-111A data analysis has been continuing inhouse and will be reported in a NASA TN. The final reports by General Dynamics on the calculation of buffet response of the F-111A are being reviewed with anticipated release by mid-1976 (NAS2-7091). One wind-tunnel model test was completed in September 1975 and preparations are in progress for another, both of the Northrop F-5A to obtain data for correlation with previously completed F-5A flight buffet data (NAS2-8734). This second wind-tunnel model test, scheduled for April 1976, will encompass a special model mounting technique which will allow controlled freedom in roll to study the fluctuating pressure characteristics associated with wing rock. The joint NASA/USAF TACT Program is progressing with 75% of the flight fluctuating pressure data having been acquired. The associated semispan model wind-tunnel tests of steel and aluminum wings which will provide information on the effects of flexibility on the fluctuating pressures that cause buffet are scheduled for May 1976. An inhouse effort has been initiated to demonstrate the application of NASTRAN for calculation of aircraft response characteristics using as inputs the fluctuating pressure power spectral and cross-spectral characteristics obtained from wind-tunnel model tests.

(Dennis Riddle, FAS)

Pressure Fluctuations Underlying Attached and Separated Turbulent Boundary Layers Since the last meeting of the RTAC the primary efforts in this area have been to support tests involving space shuttle configurations. Wind tunnel tests of a 3.5 percent scale model of the launch configuration have been completed in the Ames 9- by 7-foot Supersonic Wind Tunnel and the 11-foot Transonic Wind Tunnel at Mach numbers from 0.6 to 2.5. The model contained 240 dynamic pressure transducers to provide extensive definition of the surface dynamic loads during the launch phase of flight. A digital minicomputer was used for the first time on these tests for control of the experiments including model angles of attack and sideslip and the dynamic data acquisition and recording. The computer also allowed on-line analysis of broadband rms pressures and print out of both model and full-scale dynamic loads. The ability to record the large quantity of data combined with the computer control of the experiments yielded approximately a 10 to 1 improvement in data acquisition rate and a corresponding saving of electrical energy for wind tunnel power that otherwise would have been required to obtain the same quantity of data.

Tests have also recently been completed of large rectangular panels covered with non-rigid reusable surface insulation (NOMEX Felt RSI) with exposure to supersonic attached boundary layers to check for membrane flutter and supersonic separated flow and shock waves for exposure to high aeroacoustic dynamic loads. The panels were tested to 150 percent of flight dynamic pressure without flutter failure and to approximately 158 dB OASPL in the separated flow and 167 dB OASPL in the shock wave region with only slight local deterioration of the surface.

(Richard Hanly, FAS)

Aero-Optical Interactions The purpose of this research is to predict and minimize the disturbances in the vicinity of open ports through which electromagnetic radiation is to be passed into or out of an airplane flying at transonic speeds. The disturbances include pressure fluctuations which shake the optical elements and also the density fluctuations which distort the electromagnetic waves.

Previous reports have summarized efforts to measure and minimize the pressure disturbances, using various combinations of porous spoilers, porous cavity walls, sound-absorbing linings, and air injection. These measurements have been extrapolated to full scale with demonstrated success. However, it is not clear that optical measurements can be similarly scaled, and it is doubtful that the devices for minimizing cavity pressure fluctuations are suitable for controlling the density fluctuations.

Initial tests aimed at the optical problem have been reported since the last RTAC meeting (Refs. 1 and 2). Basic boundary-layer flow was investigated and also a flow behind a porous spoiler such as might be used to control cavity resonance. Plans are now being finalized for repeat tests of these two flows using improved instrumentation. In addition, the tests are to include a cavity protected from resonating by a porous spoiler or, alternatively, air injection into the cavity. The instrumentation will include a hot wire and laser-doppler velocimeter with outputs combined in real time to give density fluctuations with a minimum of assumptions. Other measurements will be pressure, temperature, air forces on a ball probe, and degradation of a laser beam traversing the flow.

Concurrently, tests are being planned of a model of the pointing system on the Air Force Airborne Laser Lab. One objective will be to obtain loads data with an improved fairing design;a second objective will be to measure optical degradations for correlation with those measured on the airplane.

References:

1. Van Kuren, James T.: "Experiments to Develop a Thick Turbulent Boundary Layer for Optical Degradation Measurements", AFFDL-TM-75-106-FX, June, 1975.

2. Otten, L. J., and Van Kuren, J. T.: "Artificial Thickening of Transonic Boundary Layers", AIAA Paper 76-51.

(Donald Buell, FAS)

Chemical Research Projects Office

1. Fire-Safe Materials for Aircraft Interiors
2. Laser Resistant Materials Effects Program
3. Advanced Supersonic Aircraft Fuel Tank Sealants
4. Aircraft Fuel Tank Baffle Materials
5. Elastomers for Aircraft Tires

Fire-Safe Materials for Aircraft Interiors:

(a) Interior Panels

Various types of fire-resistant composites have been fabricated for fire, smoke and toxicity testing. These composite panels are being evaluated as possible replacements of the currently used interior panels in wide body jet aircraft. Composites evaluated included (a) the baseline composite consisting of polyvinyl fluoride film on epoxy-glass bonded to a phenolic impregnated polyimide paper honeycomb (b) polybenzimidasole-glass face sheet with interconnecting truss structure (c) same as "b" but filled with polybenzimidazole foam and (d) bismaleimide-glass flat face sheets bonded to a phenolic impregnated polyimide paper honeycomb with polyimide adhesive. The honeycomb voids were filled with polyquinoxaline foam. Thermal efficiency tests were conducted on the Ames T-3 facility with a JP-4 fuel fire and a heat flux of 10 $Btu/ft^2/sec$. The test results show that the composite with the polyquinoxaline foam filled honeycomb exhibited much lower back-face temperature (greater fire endurance) than the other composite systems, especially the baseline material. Smoke tests were performed in the NBS smoke chamber using both the flaming and non-flaming test conditions. Composites fabricated from the polybenzimidazole laminate and foam produced the lowest specific optical density (D_s), followed by the sample containing the polyquinoxaline foam and the baseline material. Typical properties of the composites are shown on the attached table.

(b) Transparent Dust Cover Windows

Block polymers consisting of 9,9-bis(4-hydroxyphenyl) fluorene polycarbonate poly-(dimethylsiloxane) (BPFC-DMS) are being considered as a possible replacement to the fire-retardant acrylic (PMMA) (Rohm and Hass FI-3) pane currently used as the interior dust cover of aircraft windows. Block polymers in the form of sheets, containing alternative 9,9-bis(4-hydroxyphenyl) fluorene (BPF) polycarbonate and poly (dimethylsiloxane) (BPFC-DMS), are currently being procured from General Electric for evaluation in-house and at Boeing. The BPFC-DMS transparencies have been previously prepared for the Naval Air Systems Command. These polymers showed good retention of tensile properties at 200°C: $\simeq$ -80% of yield stress: $\simeq$ -45% of tensile strength and $\simeq$ +600% of ultimate elongation. Molding processes are being evaluated to mold these transparencies with the least amount of discoloration and with optimum thermophysical properties. Typical thermal properties are shown on the attached figure.

(D. Kourtides)

PROPERTIES OF COMPOSITES

TEST	NOMEX-EPOXY	PBI/PBI	P.Q. BISMALEIMIDE
AREA DENSITY, 2.54 cm (1 in.) THICK	2.80 Kg/m² (.577 lb/ft²)	3.3 Kg/m² (.687 lb/ft²)	2.87 Kg/m² (.588 lb/ft²)
FIRE CONTAINMENT - NASA T-3 10-11 BTU/ft²/sec, TIME TO BACKFACE TEMP. OF 477°K (400°F)	120 sec.	195 sec.	480 sec.
SMOKE DENSITY, NBS, D_s 4 min.	53.2	0	12.8
FLATWISE TENSILE, ASTM 297 KN/m² (psi)			
ROOM TEMP	1407 (214)	96 (13.9)	691 (100)
344K (160°F)	845 (122)	75 (10.8)	558 (81)

EFFECT OF TEMPERATURE ON WEIGHT LOSS OF PMMA AND BPFC-DMS

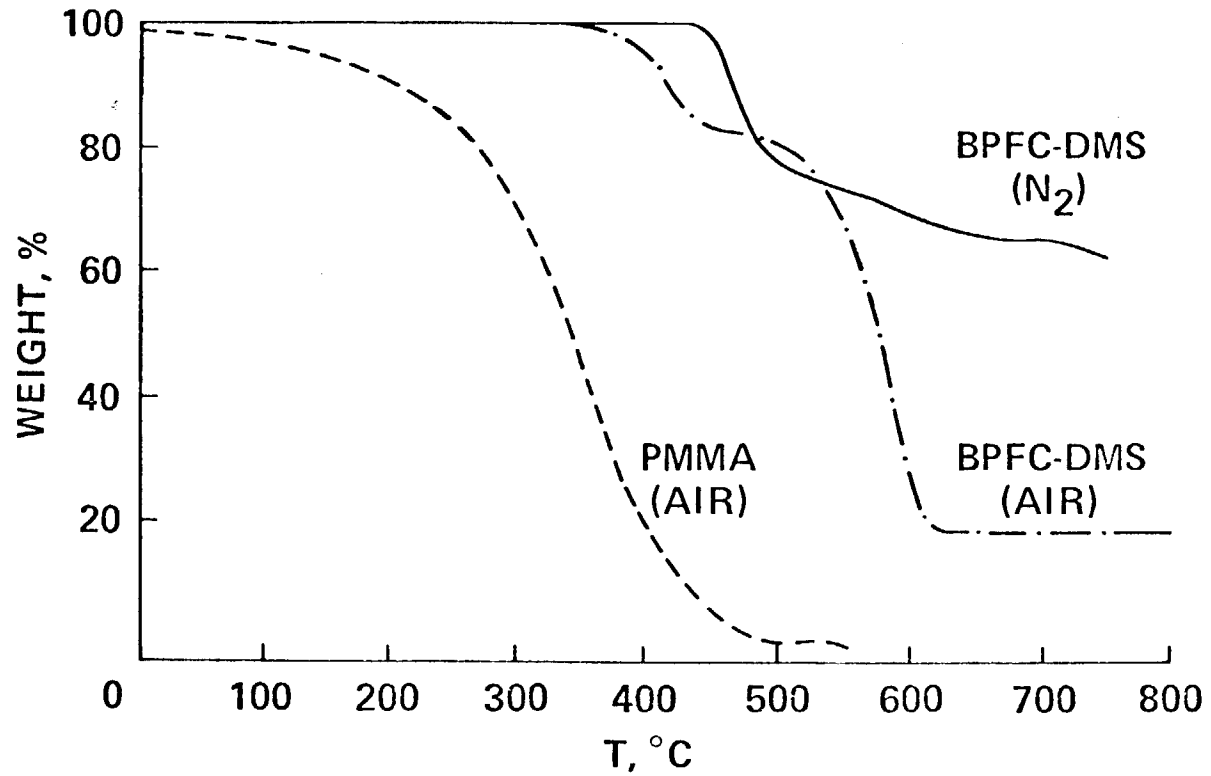

Laser Resistant Materials Effects Program. As reported, the laser effects study on NASA developed transparent materials has been completed. New studies to understand the basic relationship between polymer structure and laser environment performance have been initiated. Early experiments indicate that a relationship does exist, however, further data is required at varying intensities to confirm the results.

In addition to the basic experimental studies, an analytical study is anticipated to provide a code to predict material performance in various environments using the basic thermal chemical kinetic parameter of a polymeric material. This effort is scheduled for initiation this coming quarter.

(S. R. Riccitiello)

Advanced Supersonic Aircraft Fuel Tank Sealants. Test specimens of various fluorosilicone sealants installed in the YF-12A aircraft fuel tanks in 1975 are currently being flight tested. More than 30 flights of 2-3 hours duration each have been made and Phase 1 is now near completion. Boeing and JPL will examine the test samples for adhesion, weight, and volume loss, and stress in February or March 1976.

Preliminary results indicate the emergence of two new promising sealant elastomer candidates which will be thoroughly screened and optimized. The candidates are a fully fluorinated ether triazine and what appears to be a fully fluorinated ether 1,2,4 oxadiazole. The latter is being carefully examined and model compounds are being prepared to help in structural identification. Molecular weights are being increased selectively and several cross-link methods are being studied. These represent essential steps in ultimately achieving the appropriate physical properties suitable for a supersonic fuel tank sealant application.

(R. Rosser)

Aircraft Fuel Tank Baffle Materials. Studies of uncoated reticulated foam and that coated with Astrocoate 8000 have been completed. Side by side comparisons of fuel swell-volume changes under varying conditions were made. The final report has been submitted and approved.

(R. Rosser)

Elastomers for Aircraft Tires The goal of improved aircraft tire treads continues to be pursued by fundamental and developmental work on various tire elastomers: natural rubber (NR) or cis-1, 4-polyisoprene, cis-1, 4-polybutadiene (CB), vinyl or 1,2-polybutadiene (VB), and trans polypentenamer (TP). As an extension of last year's spectroscopic study of the thermal oxidation of polyisoprene (NR and its synthetic counterpart), an analogous examination of the thermal oxidation of CB as well as the photo-oxidation of NR is being undertaken. This work, in turn, will lead into a similar examination of VB and TP, so as to conclude a comparative oxidative investigation of all the important tire elastomers. In related fundamental work, chemiluminescence has been investigated as a potential new tool for detecting and following extremely slow (ambient) oxidative degradation of aircraft tire elastomers. Also, the basic abrasive wear mechanisms for tread elastomers are being explored. Along developmental lines, the extensive testing of the set of 75/25 NR/VB-retreaded tires (for main landing gear of Boeing 727) is making satisfactory progress. Runway tests on several of these tires have been completed and the data are being reduced. The general observation is that the NASA-Ames tires appear to perform better than the control (75/25 NR/CB) and the Air Force-developed tire (Alfin 85/15 butadiene-styrene copolymer). Other tires in the set are being flight evaluated by the FAA. Additional VB rubber has been ordered for use in retreading a new set of 50 tires for statistical evaluation of the NR/VB tread formulation in actual commercial airline service. Work is also proceeding on a new NR/TP formulation leading to the fabrication of an initial 12 tires for runway testing at Langley and flight testing by the FAA.

(M. A. Golub)

IMPROVED ELASTOMERS FOR AIRCRAFT TIRES

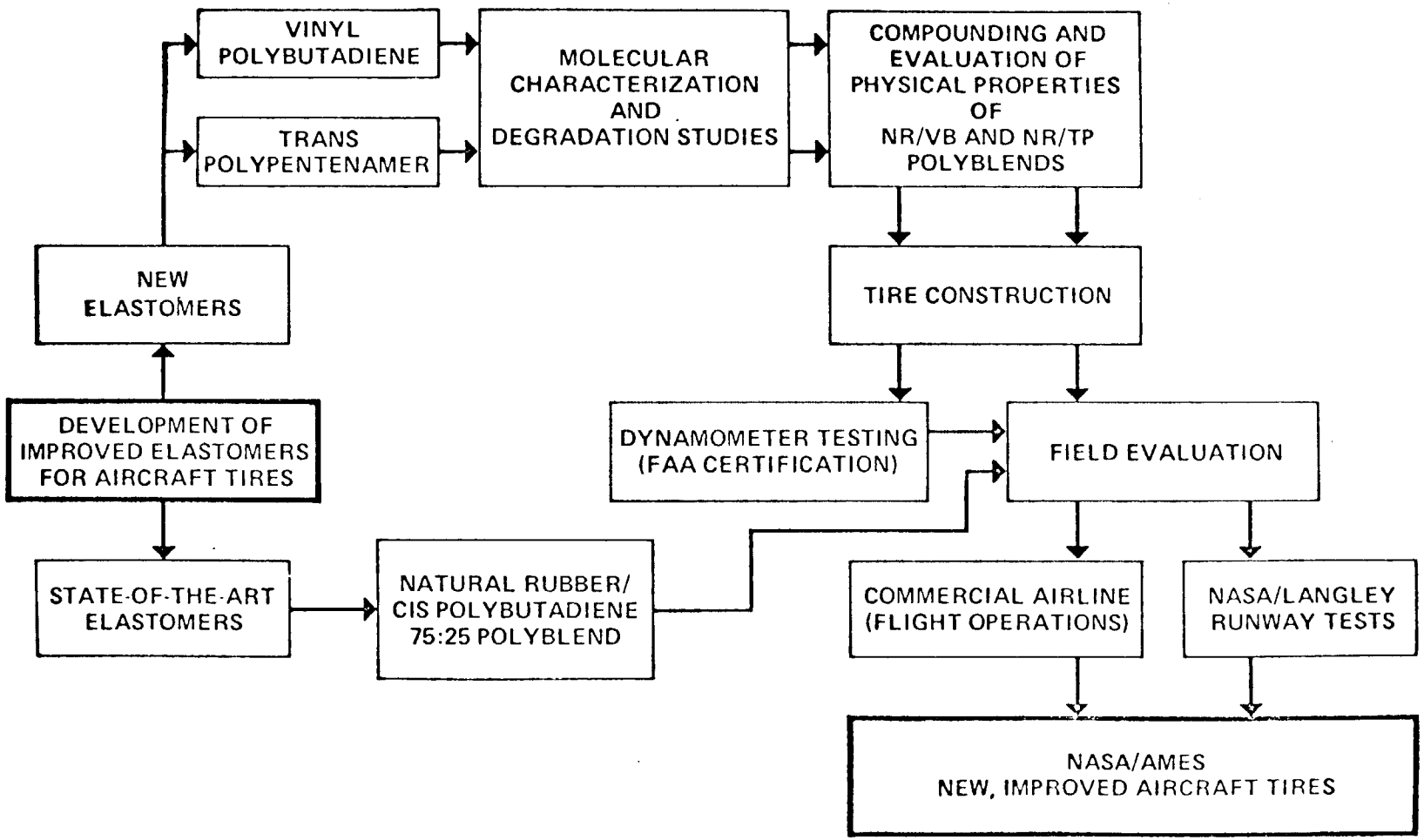

RTAC 75-2

Physical Gasdynamics and Lasers Branch

1. Band Structure Calculation of Crystalline Solids by the Empirical Pseudo Potential Method

2. Surface Reactions by the Xα-Scattered Wave Method

3. Atomic Electron Binding Energies

4. Quantum Mechanical Calculation of Fe-H and Fe-Fe Interaction Potentials

Band Structure Calculation of Crystalline Solids by the Empirical Pseudo Potential Method. Band structure calculations of the II-VI semiconductor CdSe and the transition metals Ni, V, Ta, Mo and W have been completed. Agreement between the properties calculated to date and the available experimental data are very good. This material has been or will be covered in three oral presentations at APS meetings and is contained in four scientific papers in preparation. The future direction of this research will be to develop additional computer programs to calculate other important physical properties such as the electronic charge distribution and the electron-phonon coupling. Once these programs are completed a project to calculate the properties of various alloys of the transition metals will be initiated. The purpose of this work will be to search for materials with a high critical temperature for superconductivity.

(Dr. Champa Sridhar, NRC Associate, Prof. Ching Fong, U. C. Davis, and Dr. Ellis Whiting, Ames)

Surface Reactions by the Xα-Scattered Wave Method. The Xα-Scattered Wave method is being investigated for its applicability to chemisorption and catalysis studies. Preliminary calculations for H on Ni and for CO on Cu are underway. The metal surfaces are approximated by a small cluster of five atoms and the energy of the system is calculated as a function of the distance (d) of the adsorbate specie from the cluster surface (see attached figure for H-Ni). It is hoped that this method can account for the structure in the photo emission spectra measured for such materials. In addition, the possibility of calculating the properties of small (10 Å) platinum particles by a cluster of platinum atoms is being investigated.

(Dr. Hsi-Ling Yu, NRC Associate and Dr. Ellis Whiting, Ames)

Atomic Electron Binding Energies. A complete set of relaxed-orbital electron binding energies has been calculated relativistically for atoms from He through Element 106. Each binding energy is determined as the difference between separately computed self-consistent field results for the neutral atom and for the ion; the adjustment of all remaining electron states to the vacancy is thereby taken into account. It has been known for several years that this approach leads to better agreement with precision experiments than the traditional "frozen orbital" calculations. The project was made feasible by using relativistic Hartree-Fock-Slater wave functions as

zeroth-order eigenfunctions to compute the expectation value of the total Hamiltonian. A first-order correction to the local approximation is thus made without incurring the prohibitive cost of a large number of Hartee-Fock calculations, yet with results of comparable accuracy. In addition to binding energies, the following quantities are tabulated: total energies, electron kinetic energies, electron-nucleus potential energies consisting of electrostatic and Breit interaction terms, vacuum polarization energies, and 1s self energies. A separate listing of Slater integrals is being compiled. These results will form the basis for computations of inner-shell transition rates and relativistic fluorescence yields and are likely to be applied extensively in the interpretation of Auger and X-ray photo-electron spectrometric data.

(Prof. Bernd Craseman, Univ. of Oregon, Eugene and Dr. Hans Mark, Ames)

Quantum Mechanical Calculation of Fe-H and Fe-Fe Interaction Potentials.

The computer code developed at Battelle to solve for the loosely bound or valence electronic structure and interatomic forces of Fe-H cells consisting of 6 to 10 Fe atoms and 1 or 2 H atoms has produced initial results. These preliminary data for the interatomic forces are given in Table 1 and correspond to the 10 iron atom geometry specified in Figure 1. This geometry is typical of those in the crack tip regions considered in P. Gehlen's computer simulations of crack propagation in hydrogen embrittled iron.

The calculation of the interatomic forces proceeds in two principal steps: (1) Evaluation of about 2.5 million $1/r^3$ integrals over the Gaussian type basis set, and (2) evaluation of the electron density function. The initial code for step (1) proved to be slow, requiring one hour and 16 minutes on a CDC 6400. Consequently, a new code was written, and the current time to compute the integrals is 4 minutes, which will drop further to about 0.2 minutes on the Ames CDC 7600. This new efficient code makes a study of a considerable number of pertinent geometries tractable. Step (2) is currently being performed in the "Extended Huckel Approximation" and current work is underway to perform this step by the more accurate Hartree-Fock method.

(Dr. L. Kahn, Battelle, and Dr. J. O. Arnold, Ames)

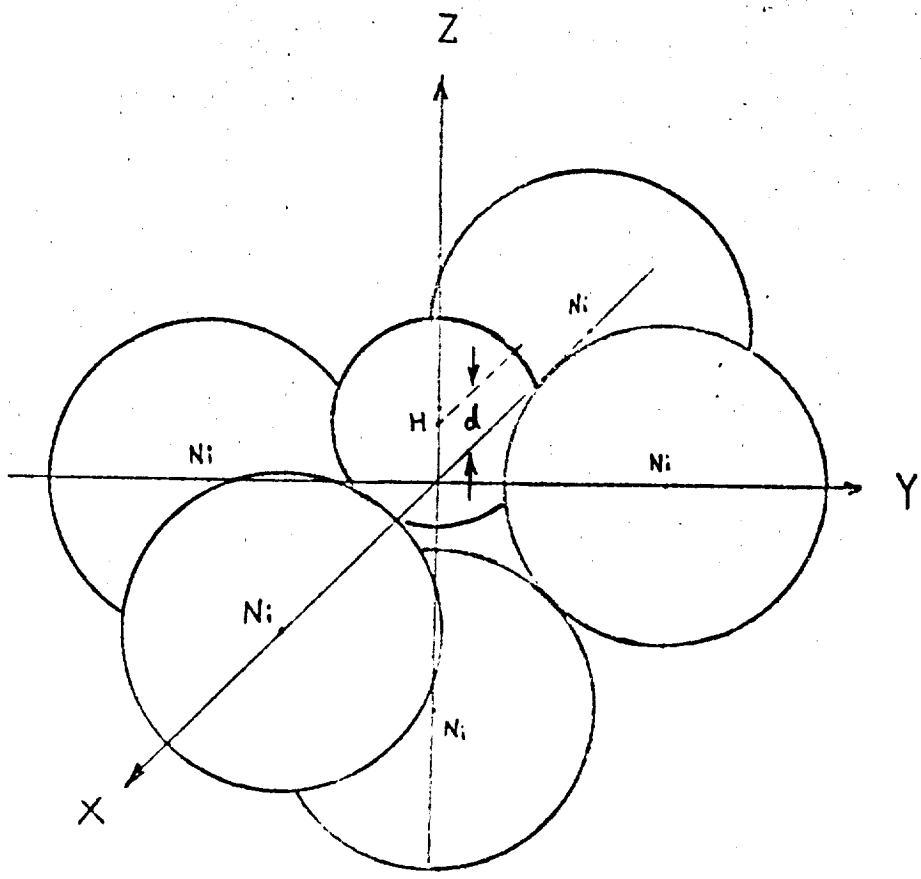
Z
Y
X
Ni
Ni
Ni
Ni
Ni
H
d

TABLE I.

CALCULATED FORCES ON THE ATOMS IN THE CLUSTER*

I	ATOM	X	Y	Z	F-X	F-Y	F-Z
1	FE	-1.4251199	-1.9653568	-2.7023656	-.1835010E-01	-.9227832E-01	-.1737438E+00
2	FE	-2.4000036	3.5905557	-2.7023656	-.4638996E-01	.1486002E+00	-.1554365E+00
3	FE	-5.8582751	5.9338657	0.0000000	-.1693256E+00	.1723680E+00	.6092512E-01
4	FE	-4.7244154	.4724415	0.0000000	-.1955193E+00	.9711526E-02	.1246383E+00
5	FE	-4.3.86668	-4.9511873	0.0000000	-.1498389E+00	-.2091527E+00	.8009709E-01
6	FE	1.4302223	-4.8189037	0.0000000	.3671366E-02	-.2174670E+00	.1282555E+00
7	FE	1.3085059	.8692924	0.0000000	.1821536E-01	.5307010E-01	.1711258E+00
8	FE	3.1937048	6.4441026	0.0000000	.2932409E-02	.2108479E+00	.1093525E+00
9	FE	4.4220528	-2.1921287	-2.7023656	.1873763E+00	-.1031710E+00	-.1612371E+00
10	FE	5.2535499	3.1370118	-2.7023656	.1728353E+00	.5627201E-01	-.1293681E+00

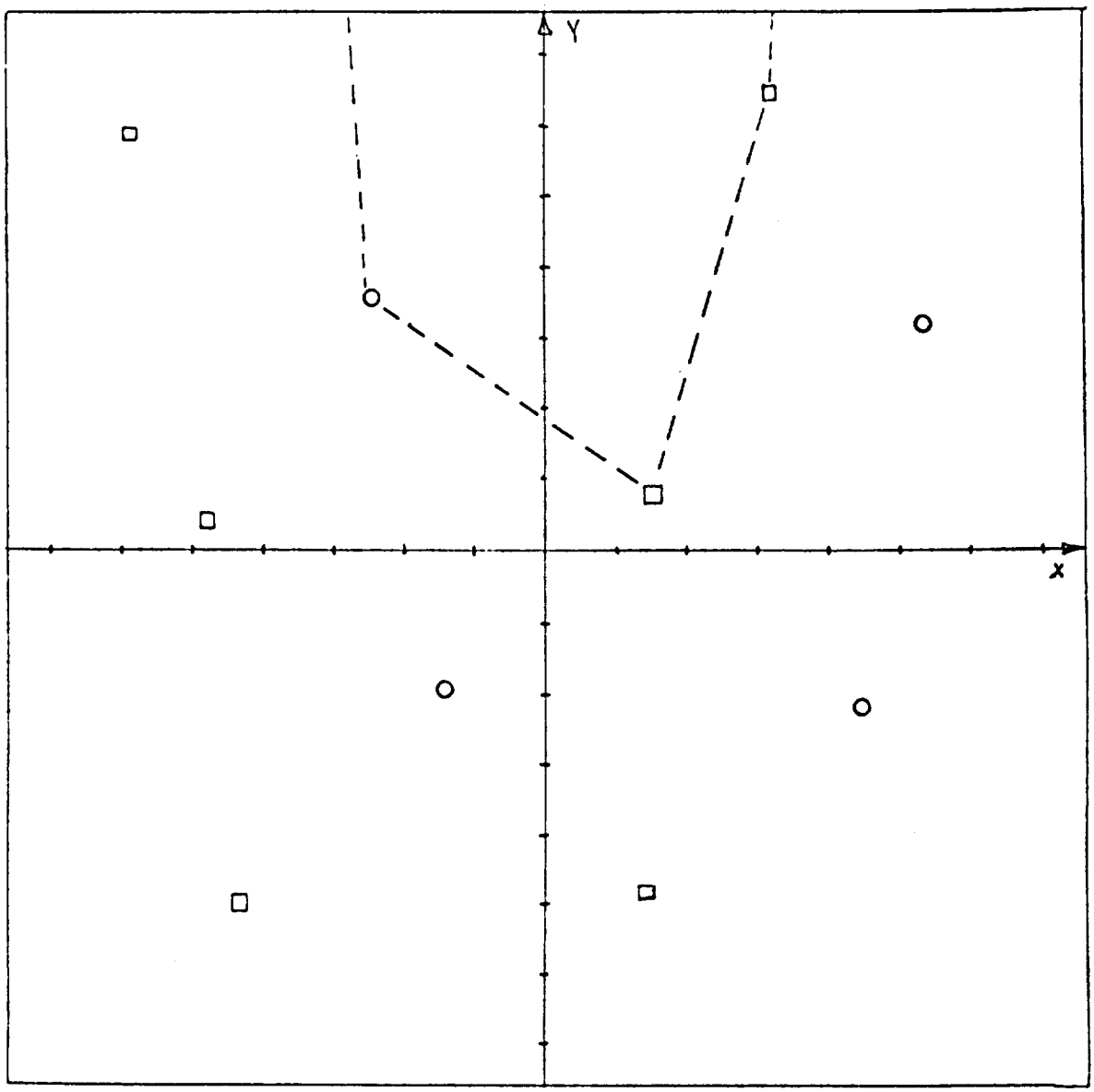

FIGURE 1.- The configuration $(\underset{\sim}{R}_1, \ldots, \underset{\sim}{R}_n)$ of the 10 Iron atoms (taken from the crack tip region of a previous computer simulation run) which was used in the interatomic force calculation of Table 1. The atoms identified by the symbols ○ and □ are in different planes specified by Z=-2.70 and 0.00. All distances are given in bohr units.

Materials Science Branch

1. Oxide Removal and Desorption of Oxygen from Partly Oxidized Thin Films of Copper at Low Pressures

2. Corrosion of 310 Stainless Steel at Elevated Temperatures in a Hydrogen Sulfide Containing Environment

3. High Temperature Hydrogen Attack of a Plain Carbon Steel by High Purity Hydrogen

4. Slow Crack Growth of Zircaloy-4 in a Gaseous Hydrogen Environment

5. Direct Observation of Small Cluster Mobility and Ripening

6. A Computer Study of Various Factors Affecting the Nature of Surface Deposition

7. Formation Mechanism for Multiply Twinned Particles During Nucleation in the Au/Mica System

8. The Kinetics of Hydrogen Chemisorption onto Evaporated Iron Films

9. Failure and Fracture Behavior of Graphite/Epoxy Laminates

10. Computer Modeling Analysis of the Fracture of Fiber Reinforced Composites

11. Fatigue of Angle-Ply Graphite/Epoxy Composites

Oxide Removal and Desorption of Oxygen from Partly Oxidized Thin Films of Copper at Low Pressures. Partly oxidized copper films were annealed in a controlled vacuum (> 10^{-9} Torr) at 450°C. The changes were observed *"in-situ"* with a specially designed high-resolution transmission electron microscope. The thin, (100)-oriented, mono-crystalline films of copper had been oxidized immediately prior to the annealing studies at the same temperature and at an oxygen partial pressure of 5×10^{-3} Torr, until the desired fraction of the copper film was converted to oxide. It was observed that the oxide disappeared during annealing as long as some copper was left unoxidized. The disappearance of the oxide was explained by a mechanism involving dissociation of oxide at the oxide/metal interface followed by diffusion of oxygen into the metal and desorption of oxygen from the surface of the unoxidized copper. The rate of disappearance of the oxide was found to be proportional to the surface area of unoxidized copper. In the case of heavily oxidized films (> 50%), some holes developed in the oxide near the oxide/metal interface after an annealing period of two to three hours. Upon resumption of the oxidation, the pinholes first disappeared, and normal oxidation behavior was observed. The formation of holes may be explained by vacancy clustering. When completely oxidized films were annealed, recrystallization of the oxide was observed.

(D. B. Rao, K. Heinemann, D. L. Douglass)

Corrosion of 310 Stainless Steel at Elevated Temperatures in a Hydrogen Sulfide Containing Environment. Corrosion of 310 stainless steel in a gaseous mixture containing argon and hydrogen sulfide (P_{S_2} = 8.9×10^{-3} atms) was studied in the temperature range of 600° - 1000°C. At temperatures below approximately 870°C, the rate of growth of corrosion product was controlled by a parabolic rate law having an activation energy similar to the literature value for the diffusion of iron through iron sulfide. At temperatures of 970°C and above the rate law became linear. A systematic examination of the corrosion products revealed the presence of duplex scales. At the lower temperatures an outer scale formed of $Fe_{(1-X)}S$ (X=0.094) with some amount of dissolved nickel. This outer scale was followed by a thin subscale composed of a mixture of iron-chromium and nickel-chromium sulfides ($FeCr_2S_4$ and $NiCr_2S_4$). The scale which directly adhered to the alloy was composed of Cr_2S_3. At higher temperatures some liquid sulfide was detected at the outer scale as separate islands with the melt extending through the grain-boundaries. Energy dispersive x-ray analysis

indicated that the liquid mainly consisted of iron and nickel sulfides and whose exact composition has yet to be determined. The diffusion of chromium to the outer scale was found to increase with increasing temperature.

(D. B. Rao, Howard G. Nelson)

High Temperature Hydrogen Attack of a Plain Carbon Steel by High Purity Hydrogen. The degradation of a plain carbon steel exposed to high purity hydrogen at high temperatures was studied in an effort to establish: 1) The influence of material thickness (the influence of normal hydrogen transport processes); 2) the influence of a strain gradient; and 3) whether or not there are additional hydrogen associated processes which may enhance attack (the formation of H_2S at sulfide rich areas, etc.). SAE 1020 steel coupons having a range of thicknesses from 0.010 in. to 0.5 in. were exposed to 500 psi hydrogen over the temperature range from 300°C to 600°C for various times. The degradation in room temperature mechanical properties was found to be independent of specimen thickness or distance from coupon surface suggesting the rate of hydrogen attack is independent of hydrogen transport processes -- sufficient hydrogen was present at all times. A strain gradient was found not to influence the rate of attack; however, a strain concentrator (crack) had a significant influence. Finally, CH_4 was the sole species found during the fracture of exposed specimens. No other species such as H_2S were observed.

(Howard G. Nelson and R. Dale Moorhead)

Slow Crack Growth of Zircaloy-4 in a Gaseous Hydrogen Environment. The slow crack growth behavior of annealed Zircaloy-4 plate was studied in a high purity gaseous hydrogen environment as a function of applied stress intensity (K), hydrogen pressure, and temperature. Compact tension-type specimens were machined from material having the basal poles aligned at about 30 degrees to the normal to the plate in the plane defined by the normal and transverse directions. At all pressures and temperatures investigated, crack growth as a function of K was found to be similar to that commonly observed for other forms of stress corrosion cracking -- a threshold stress intensity below which crack growth is not observed, a rapid increase in crack growth as K is increased (Stage I) and a region of constant crack growth rate with a

further increase in K (Stage II). Increasing hydrogen pressure from 6.7 kN m^{-2} to 86.2 kN m^{-2} was found to decrease the threshold stress intensity and increase the rate of slow crack growth in Stage II. The plateau slow crack growth rate of Stage II was found to be proportional to the square root of the hydrogen pressure. Increasing temperature from 23°C to 70°C was found to increase both the threshold stress intensity and the rate of Stage II crack growth. These observations together with a detailed analysis of the fracture surfaces suggest that hydrogen-induced slow crack growth in Zircaloy-4 is controlled by the rate of hydrogen transport in the zirconium lattice.

(Harry Wachob and Howard G. Nelson)

Direct Observation of Small Cluster Mobility and Ripening. New, direct evidence has been found for the simultaneous occurrence of Ostwald ripening and short-distance cluster mobility during annealing of discontinuous metal films on clean amorphous substrates. The annealing characteristics of very thin particulate deposits of silver on amorphized clean surfaces of single crystalline thin graphite substrates have been studied by *in-situ* transmission electron microscopy (TEM) under controlled environmental conditions (residual gas pressure of 10^{-9} torr) in the temperature range from 25 to 450°C. It was possible to monitor all stages of the experiments (i.e., sputter cleaning of the substrate surface, metal deposition, and annealing) by TEM observation of the same specimen area. Various techniques (e.g., pseudosterographic presentation of micrographs in different annealing stages, the observation of the annealing behavior at cast shadow edges, and measurements with an electronic image analyzing system) were employed to aid the visual perception and the analysis of changes in deposit structure recorded during annealing. Slow Ostwald ripening was found to occur in the entire temperature range, but the overriding surface transport mechanism was short-distance cluster mobility. This was concluded from *in-situ* observations of individual particles during annealing and from measurements of cluster size distributions, cluster number densities, area coverages, and mean cluster diameters.

(K. Heinemann and H. Poppa)

A Computer Study of Various Factors Affecting the Nature of Surface Deposition. In this investigation it has been shown that the structure and the shape of a surface deposit can, in principle, be calculated from the physical properties of atoms involved (i.e., adatoms and substrate atoms). To

calculate interaction energies among atoms a Lennard-Jones type potential was considered. First, a simple approach was developed to calculate Lennard-Jones potential parameters for metals using only crystalline state physical properties. The structure and the shape of an epitaxial overgrowth was then calculated by minimizing the energy of interaction of the adatom-substrate system. The most probable configuration of adatoms in the deposit was expressed in terms of physical properties of atoms involved. Numerical test for one-dimensional surfaces indicate that the method is able to reproduce all basic growth mechanisms encountered in experiments.

(T. Halicioglu and H. Poppa)

Formation Mechanism for Multiply Twinned Particles During Nucleation in the Au/Mica System. The formation of thin films of gold on mica has been studied in ultra-high vacuum ($5X10^{-10}$ torr). The mica substrates were heat-treated for 24 hours at 375°C, cleaved, and annealed for 15 minutes at the deposition temperature of 300°C prior to deposition. An impingement flux of $3X10^{13}$ atoms cm^{-2} sec^{-1} was used. These conditions were found to give high number densities of multiple twin particles and are based on a systematic series of nucleation experiments described elsewhere. Individual deposits of varying deposition time were made and examined by bright and dark field TEM after "cleavage preparation" of high transparent specimens. In the early stages of growth, the films generally consist of small particles which are either single crystals or multiply twinned; a strong preference for multiply twinned particles (MTP's) was found whenever the particle number densities were high. The time period of fastest increase in MTP-particle density was found to coincide with the period of fastest decrease in single crystal particle density, which indicates formation of MTP's by coalescence of single crystal particles. For this result, single and multiple twin particles had to be distinguished. This was possible on the basis of shape for large crystallites (> 90 sec) only. For the classification of small crystallites, it was often impossible to rely on a simple shape criterion. The distinction, however, is easily made with the method of selected zone dark field microscopy (SZDF). The SZDF study also indicates clearly that the single crystal particles nucleate initially and that the multiple twin particles are formed somewhat later, resulting from migration coalescence of single crystals. The latter process starts within less than 5 sec after deposition starts. TED pattersn also confirm the sharp increase with increasing deposition time of the number densities of (epitaxially oriented) multiply-twinned particles:

the respective (111)-reflections are increasingly enhanced. We conclude, therefore, that early coalescence of migrating small crystallites with high surface mobilities is responsible for the generation of multiply twinned particles in this case. They are not formed in a nucleation event as, for instance, suggested by Komoda for gold on sodium chloride. High number densities are a further prerequisite for such early coalescence events to occur frequently, in spite of the relatively large surface mobilities which are found for the small and growing crystallites (50 to 100 Å in diameter).

(E. Lee and H. Poppa)

The Kinetics of Hydrogen Chemisorption onto Evaporated Iron Films. Additional measurements and analyses have been made of the isothermal adsorption - desorption kinetics for H_2 chemisorbed onto Fe films. As previously reported the chemisorption process is observed to proceed via a precursor state of adsorbed molecular hydrogen. A mathematical model describing this physical process has been solved numerically with excellent agreement between the adsorption measurements and the computations. The reaction step connecting the precursor state with the chemisorbed state can, under certain conditions, be the rate limiting step for adsorption. The activation energy for this process is being investigated in more detail with preliminary results in good agreement with other related work. Surface poisoning, noted in the earlier work, has been determined to arise from certain impurities which are present on the substrate and diffuse through the evaporated Fe film to its free surface where they either react among themselves or with the adsorbed hydrogen, the Fe acting as a catalyst.

(M.R. Shanabarger)

Failure and Fracture Behavior of Graphite/Epoxy Laminates. The first phase of an experimental investigation to define the failure and fracture characteristics of AS/3501 graphite-epoxy laminates has recently been completed. Test were conducted on both unidirectional $(0)_{8s}$ and angle-ply $(0/\pm30/0)_{2s}$ materials in the unnotched and notched conditions. Tension tests were performed on unnotched specimens at various inclinations to the fiber directions in order to test the usefulness of lamination theory and various transformation relationships in predicting tensile moduli. On the basis of these tests it was concluded that use of orthotropic

transformation equations to predict moduli resulted in equally good results as did the use of lamination theory, expecially for angle-ply laminates.

Lamination theory was used in conjunction with the Tsai-Hill and Ashkenazi failure theories to attempt to predict failure loads. For both criteria, the predictions were quite inaccurate and attempts are currently underway to modify the failure criteria. Preliminary indications are that considerable improvement can be made by assuming that a ply is only partially lost to the laminate when the failure conditions for that ply have been reached.

Fracture tests were conducted on specimens containing a variety of types and geometries of notches. On the basis of these tests, it was indicated that both unidirectional and angle-ply materials are notch sensitive. It was found that splitting of the laminate parallel to the fibers was always the controlling fracture mode for unidirectional materials regardless of the orientation of load with respect to fiber direction. Fracture occurred generally normal to the 0° fiber in tests on $(0, \pm 30°, 0)_{2s}$ specimens when the load was in the direction of the 0° fiber; in all other cases, the fracture plane coincided with the direction of the principle fiber. Stable crack growth was noted in most tests prior to the onset of catastrophic failure. This growth appeared to occur in stages, probably first on inner plies.

The fracture results of both unidirectional and angle-ply laminates were compared with the theories generally attributed to Waddoups et al and to Whitney and Nuismer. In contrast to some earlier studies, it was found here that a closer correlation was obtained between the theoretical predictions and the unidirectional test results than the theoretical predictions and the angle-ply results. In the case of both of both of the theories, it is felt that much of the difficulty resides in the finite width correction factor which includes an orthotropic stress concentration factor. When the orthotropic factor is disregarded, good agreement is obtained between the theories and the test results. The reason for this is presently unknown.

(Brinson (VPI) - Ames contact D. Williams)

Computer Modeling Analysis of the Fracture of Fiber Reinforced Composites. A computer modeling approach is being used to attempt to correlate predicted failure loads and

failure modes with experimentally observed composite laminate failures. The objective of this work is to obtain a more basic insight into the relationships between microscopic failure events and macro-failure. The approach is to analytically imbed a local heterogeneous region surrounding the crack tip into an anisotropic elastic continuum. The intent is to have the model (1) permit an explicit analysis of the micromechanical processes involved in the fracture process, and (2) remain simple enough to be useful in practical computations. Material properties used in the analysis are being obtained from concurrent experimental programs at Ames and VPI.

Computations for arbitary flaw size and orientation under arbitrary applied load combinations have been performed for unidirectional composites with linear elastic-brittle constituent behavior. The mechanical properties were nominally those of graphite epoxy. With the rupture properties arbitrarily varied to test the capability of the model to reflect real fracture modes in fiber composites, it has been shown that fiber breakage, matrix crazing, crack bridging, matrix-fiber debonding, and axial splitting can all occur during a period of (gradually) increasing load prior to catastrophic fracture. Of most importance, the computations reveal qualitatively the sequential nature of the stable crack growth process that precedes fracture in composites. Quantitative comparisons with the VPI experimental results on edge-notched unidirectional graphite epoxy specimens have also been made and found to be in fair agreement.

(Kanninen, Rybicki (Battelle) - Ames contact D. Williams)

Fatigue of Angle-Ply Graphite/Epoxy Composites. An experimental study of the fatigue behavior of unnotched $(0/\pm 30°)_{3s}$ Gr/Ep composites has been recently completed. Unsupported test specimens were axially cycled under tension-tension, tension-compression, and compression-compression loading. The test specimens exhibited static tensile and compressive strengths of 123 and 66 ksi, respectively, due at least partially to the occurrence of a buckling failure mode in compression. That this was true could be proven by the observation that a reduction in gage length of 50% (from 2 inches to 1 inch) caused a 30% increase in compressive strength. It was found that the angle-ply composites showed a definite fatigue effect under all loading conditions as indicated by a fatigue limit - i.e., load at 10^7 cycles - which was approximately 60% of the respective static failure

stresses in tension and compression. The differences in static strengths in tension and compression were reflected in a skew-symmetry of the constant-life (Goodman) diagram; this resulted in a maximum specimen life occurring at a mean stress greater than zero.

The specimen compliance was monitored as a function of applied stress cycles and it was found that no major changes occurred until the last 10% of life. The residual strengths of several precycled specimens were measured prior to fatigue failure. No firm correlation was noted between stiffness reduction at the time of fatigue interruption and strength reduction; however, as a general rule, the reduction in strength was greater than the corresponding reduction in stiffness.

Detailed microscopic examinations were made of post-failed specimens using both optical and scanning electron microscopy. A number of axial and shear failure modes were identified from fractographic examinations and the relative amounts of these features were found to depend on the fatigue stress ratio. Subsurface cracking was found to occur extensively along directions defined by fiber/matrix interfaces.

(S. V. Ramani)

Systems Development Branch

1. Thermal Control - Heat Pipe Technology

Thermal Control - Heat Pipe Technology. The objectives of the Ames heat pipe program are (1) to establish flight-level confidence in advanced heat pipe technology through flight tests, (2) to develop basic control mechanisms, allowing variable-conductance, feedback-control, and diode operation, and (3) to develop improved liquid transport capacity and reliability. Continuing progress in all of these areas is being made.

A recent flight test of the Ames Heat Pipe Experiment aboard the Orbiting Astronomical Observatory (OA)-3) showed excellent performance after 3-1/2 years in orbit. The Advanced Thermal Control Flight Experiment on ATS-6 continues to operate well. Approval has just been obtained for a Goddard-Ames heat pipe experiment on the March 1978 TIROS-N launch. Ames will supply a high-performance cryogenic diode pipe, capable of cooling and protecting infrared detectors.

In-house investigations of basic control mechanisms include tests and analysis of a gas-controlled, grooved, cryogenic variable conductance pipe, which has showed encouraging results. Also underway are forward- and reverse-mode testing of an engineering model of the TIROS liquid-blockage diode, and operation of electrohydrodynamic heat pipes with voltage control of heat transfer.

Other programs are improving base heat pipe technology. A program to develop hydrogen heat pipes, for isothermalization of cooled optics and other applications, has just been initiated. Two flexible cryogenic heat pipes, typicsl of radiator deployment or movable detector applications, have been fabricated and are under test. Pipes with axially-varied porosity have tested successfully with fluids which cover the 100-200 K range.

Two promising techniques to improve heat pipe capacity, the "inverted meniscus" evaporative surface, and the jet-pump assisted artery, have successfully completed proof-of-principle experiments. Heat pipes incorporating these features will be designed, built, and tested. Also, digital and analog computers have been used recently in models which help explain aspects of steady and transient behavior of cryogenic heat pipes.

Communication with Air Force heat pipe users has been maintained, in accord with the OAST/AFSC interdependency agreement. Where appropriate, Air Force requirements have been factored into the OAST program.

The manpower resources of the Ames heat pipe team are currently very good. The thrust of the program continues in the direction of cryogenic temperatures, where many potential applications exist, and where advances promise to allow substantial improvements in instrument sensitivity and stability.

(Craig R. McCreight)

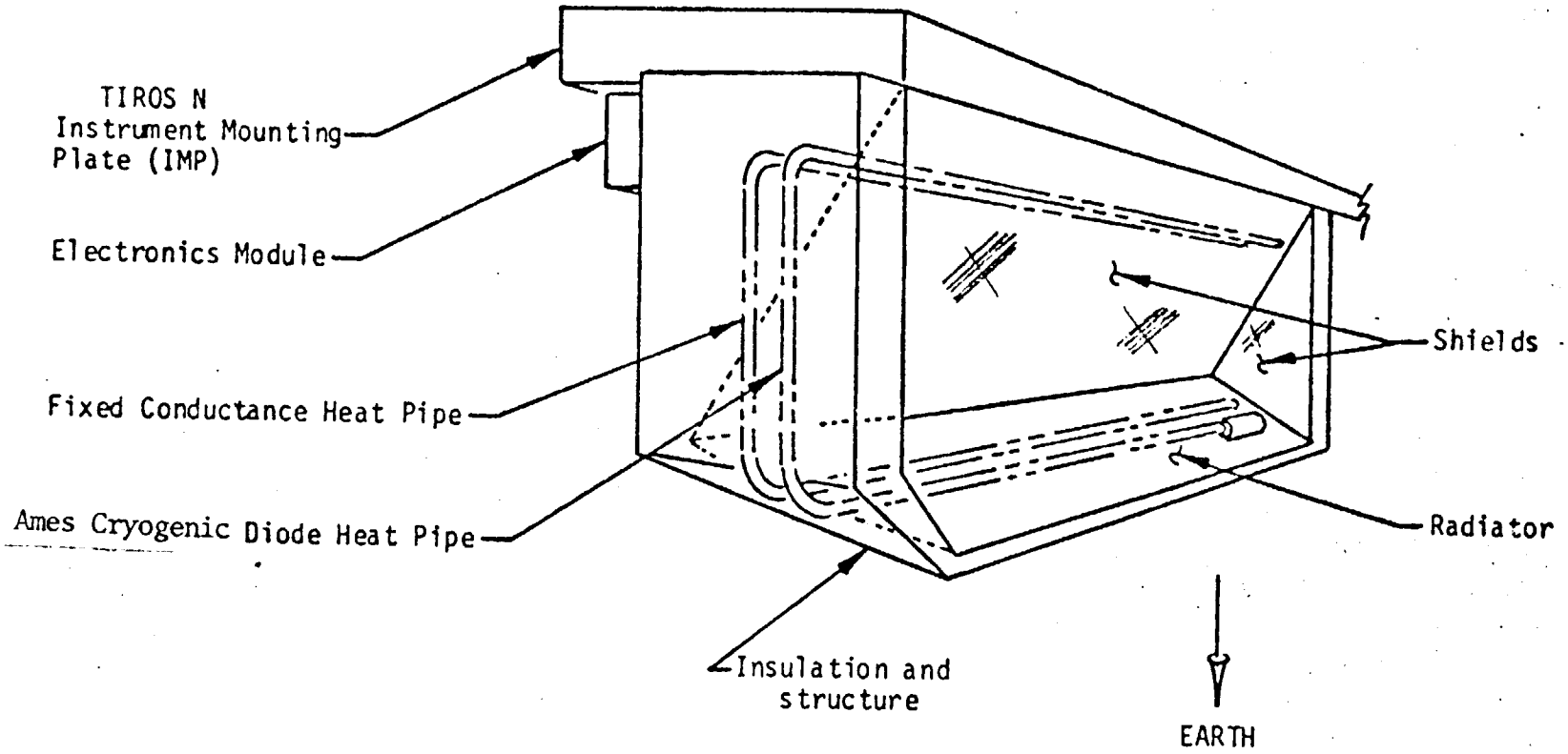

TIROS-N HEAT PIPE EXPERIMENT

Thermal Protection Branch

1. Advanced Thermal Protection Materials
2. Hyperpure Slipcast Silica Development

Advanced Thermal Protection Materials. Ames Research Center is developing improved reusable heat shield materials for advanced Space Shuttle, Earth Orbital Transportation Systems and other related applications. For the past six months we have concentrated on three programs.

In cooperation with LMSC we have scaled up the Ames Reaction Cured Glass Coating (RCG) System from a laboratory process to a semiproduction process. By direction of Rockwell International, this coating system is being evaluated at LMSC, Sunnyvale, as a backup for the current RSI (LI-0050) coating system for the Space Shuttle.

Flight tests on the X-24 B of Ames high density RSI have been completed successfully. Martin Marietta Corporation has on the basis of these and other tests adopted this material as the leading edge heat shield for their version of the X-24C. They are currently completing an internally funded program to demonstrate that they can manufacture the material by the Ames developed process.

Initial furnace and arc plasma tests are being performed on flexible blanket materials developed by Johns Manville Corporation for NASA/Ames. Initial test results indicate that one of the materials being studied having quartz cloth face sheets will have a reuse temperature on the order of 2000°F. Another material has been tested for twenty arc jet cycles with only minor damage at temperatures above 1200°F.

(Howard Goldstein)

Hyperpure Slipcast Silica Development. For future entry probe missions, especially to the outer planets, the heat shield environment is such that the amount of incident radiative flux is greater than the amount of radiation that can be emitted from the heat shield surface. To cope with this environment, Ames Research Center is developing volume reflecting heat shield technology. Previous analytic descriptions and performance evaluations in the combined radiative convective heating environment led Ames to select silica as the optimum heat shield material.

The direct application of this high purity silica material would be for use on an ablative reflective heat shield on interplanetary probes on which extremely high radiant heat fluxes will occur. Materials which have heretofore been

developed and evaluated for this purpose have been strictly of the ablative type. A high purity silica heat shield would be ablative but would also resist heating during entry due to its high reflectivity.

A previous report summarized the contractor's (McDonnell Douglas) fabrication efforts; this report describes Ames recent activity in the evaluation of the material.

The silica materials are subjected to combined radiative and convective heating in the Ames Advanced Entry Heating Simulator. The convective heating is supplied using an electric arc-jet and the radiation is supplied by means of an Argon radiation source. The spectral distribution of the source closely approximates a 6000°K blackbody, i.e., the spectral distribution of solar radiation.

The total heating seen by the ablation models was about 50/50 convective and radiation, and the combined level was as high as 5 KW/cm^2.

The accompanying figure compares the results of tests on silica with carbon phenolic (carbon phenolic is the current state-of-the-art heat shield material). The inverse slopes of the lines shown on the figure give a measure of the effective heat of ablation of the materials. In the combined heating environment, the reflecting materials indicate an effective heat of ablation twice that of carbon-phenolic. This superior performance can be traced back to the reflection of the radiation from the silica material. The reflection takes place in the interior by means of scattering so that the vaporizing ablating surface does not impede the reflection process.

(Philip Nachtsheim)

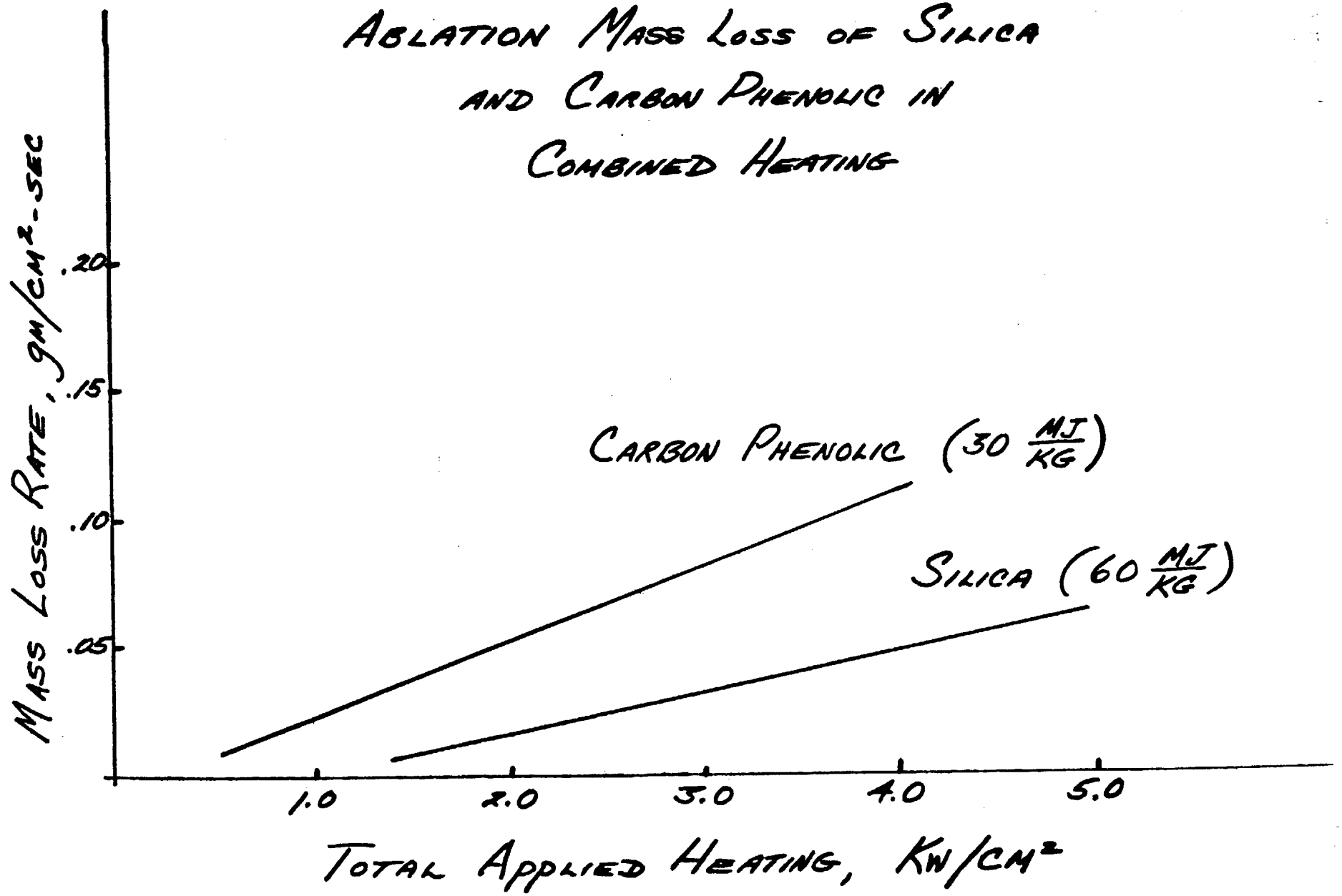
ABLATION MASS LOSS OF SILICA AND CARBON PHENOLIC IN COMBINED HEATING
MASS LOSS RATE, GM/CM²-SEC
.20
.15
.10
.05
CARBON PHENOLIC (30 MJ/KG)
SILICA (60 MJ/KG)
1.0
2.0
3.0
4.0
5.0
TOTAL APPLIED HEATING, KW/CM²